Hindawi
International Journal of Antennas and Propagation
Volume 2018, Article ID 4867851, 16 pages
https://doi.org/10.1155/2018/4867851

Research Article

An Antenna Array Sidelobe Level Reduction Approach through Invasive Weed Optimization

Geng Sun,[1,2,3] **Yanheng Liu**,[1,2] **Han Li**,[1] **Shuang Liang**,[1,4] **Aimin Wang**,[1,2] **and Boyu Li**[1]

[1]*College of Computer Science and Technology, Jilin University, Changchun, Jilin 130012, China*
[2]*Key Laboratory of Symbolic Computation and Knowledge Engineering of Ministry of Education, Jilin University, Changchun, Jilin 130012, China*
[3]*School of Electrical and Computer Engineering, Georgia Institute of Technology, Atlanta, GA 30302, USA*
[4]*Department of Information Technology, Changchun Vocational Institute of Technology, Changchun 130033, China*

Correspondence should be addressed to Aimin Wang; wang_ai_min@126.com

Received 26 July 2017; Revised 10 November 2017; Accepted 11 December 2017; Published 13 February 2018

Academic Editor: Symeon Nikolaou

The problems of synthesizing the beam patterns of the linear antenna array (LAA) and the circular antenna array (CAA) are addressed. First, an optimization problem is formulated for reducing the maximum sidelobe level (SLL) of the beam patterns. Then, the formulated problem is solved by using the invasive weed optimization (IWO) algorithm. Various simulations are performed to evaluate the effectiveness of the IWO algorithm for the synthesis of the beam patterns of the LAA and the CAA. The results show that IWO has a better performance in terms of the accuracy, the convergence rate, and the stability compared with other algorithms for the SLL reductions. Moreover, the electromagnetic simulation results also show that IWO achieves the best performance for the beam pattern synthesis of the antenna arrays in practical conditions.

1. Introduction

With the rapid development of the communication technologies and the explosive growth of the number of users, the capacity of a communication system has bottlenecks [1]. Usage of the antenna arrays can improve the capacity and the spectral efficiency of a wireless communication system [2, 3]. For example, the fifth generation (5G) communications adopt the millimeter wave (mm-wave) and beamforming technologies based on antenna arrays, to improve the spectral efficiency and communication rate of the system [4]. Moreover, the energy efficiency of a communication system can be enhanced by using the antenna arrays [5].

Beam pattern characteristic is one of the most important properties of an antenna array [6]. A directional mainlobe with the low sidelobe level (SLL) of the beam pattern will effectively enhance the communication quality and reduce the interferences [7, 8]. Thus, synthesizing the beam pattern of an antenna array is very important. The classical synthesis methods for antenna arrays, such as the perturbation methods [9], are used to optimize the beam patterns, but it requires considerable work and rich debugging experiences. Thus, practicing this method is not reliable. Moreover, existing array-weighting optimization schemes, for example, the Dolph-Chebyshev [10] and the Taylor [11] approaches, have already been tested experimentally to be an effective method to solve the beam pattern optimization problems. However, these approaches are only suitable for synthesizing the antenna arrays with less numbers of antenna elements. In addition, there are strict restrictions for using such approaches.

Swarm intelligence and evolutionary algorithms are efficient methods for the beam pattern synthesis of the antenna arrays. These algorithms are suitable for solving large-scale antenna array synthesis problems since they do not require any restrictions on antenna arrays. Todnatee and Phongcharoenpanich [12] use a method based on genetic algorithm

(GA) to synthesize the radiation pattern of a nonuniform linear antenna array (LAA), and a maximum SLL of −20 dB can be achieved by the proposed method. Chakravarthy and Rao [13] propose to use a particle swarm optimization- (PSO-) based algorithm to synthesize the beam pattern of a circular antenna array (CAA). Reference [14] also uses PSO as the optimizer to synthesize the pencil beam pattern of the time-modulated concentric circular antenna array (CCAA). Sharaqa and Dib [15] optimize the beam patterns of the CAA and the CCAA by using the firefly algorithm (FA); the excitation currents and the spacing between the elements are jointly optimized for reducing the maximum SLL. Singh and Salgotra [16] use the flower pollination algorithm (FPA) to determine the excitation currents of a LAA for reducing the maximum SLL and controlling the nulls. Li et al. [7] utilize a biogeography-based optimization (BBO) algorithm to suppress the maximum SLL of the LAA and CAA. Reference [4] also uses a BBO-based method to reduce the maximum SLL as well as to achieve the deep nulls. Saxena and Kothari [17] optimize the beam pattern of the LAA by using the grey wolf optimization (GWO) algorithm. Sun et al. [18] adopt a strategy based on cuckoo search (CS) algorithm to suppress the maximum SLL of the CCAA. The authors in [19] also use a CS-based algorithm to synthesize the beam patterns of a large-scale planar antenna array (PAA). Reference [20] utilizes the social network optimization (SNO) algorithm to design the PAA, and the results are compared with the stud genetic algorithm. Saxena and Kothari [21] use the ant lion optimization (ALO) to suppress the maximum SLL and to control the deep nulls of the LAA. In reference [22], a hybrid approach called particle swarm optimization and gravitational search algorithm-explore (PSOGSA-E) is proposed to reduce the maximum SLL of the random antenna array. Reference [23] uses the binary spider monkey optimization algorithm to design the work status of each element of the CCAA for achieving a lower maximum SLL.

In this paper, the invasive weed optimization (IWO) [24] is employed to solve the beam pattern synthesis problems of the LAA and the CAA for reducing the maximum SLL. First, we formulate a beam pattern optimization problem for reducing the maximum SLLs of the LAA and the CAA. Second, we use the IWO algorithm to solve the formulated problem. Then, the key parameters of the IWO algorithm are tuned to achieve better performance for synthesizing the beam patterns. Finally, we conduct simulations based on different numbers of antenna elements for the LAA and the CAA, respectively, to verify the effectiveness of IWO. Moreover, the electromagnetic (EM) simulations are also conducted to evaluate the beam patterns in practical conditions. The results show that IWO achieves the best performance compared with other algorithms for the LAA and the CAA optimization problems.

The rest of this paper is organized as follows. Section 2 discusses the geometries and the array factors of LAAs and CAAs. Section 3 formulates the sidelobe reduction problem. Section 4 introduces the IWO algorithm. Section 5 shows the simulation results. Section 6 summarizes the findings and concludes the paper.

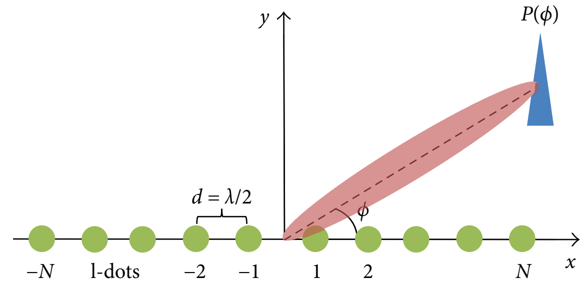

Figure 1: Geometry of $2N$-element-symmetric LAA placed along the x-axis.

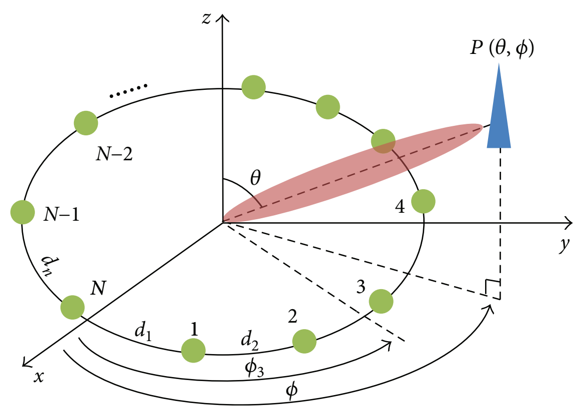

Figure 2: Geometry of a nonuniform CAA with N isotropic antennas.

2. System Model

In this section, the geometry structures and the array factors (AF) of LAA and CAA are introduced.

2.1. LAA. Figure 1 shows an LAA with $2N$ elements that are symmetrically distributed along the x-axis. The elements of the LAA are assumed as the isotropic radiators. Thus, according to the electromagnetic wave superposition principle, the AF of an LAA is expressed as follows [25]:

$$\mathrm{AF}(\phi) = \sum_{n=-N}^{N} I_n \cos(k x_n \cos(\phi) + \varphi_n), \tag{1}$$

where k represents the wave number, I_n is the excitation current of the nth element, α_n is the phase of the nth element, x_n is the location of the nth element, and ϕ is the azimuth angle measured from the positive x-axis.

2.2. CAA. Figure 2 shows the geometry of a CAA with N isotropic antenna elements lying on the x-y plane ($\theta = 90^\circ$). These elements are uniformly placed on a ring with the radius of a. Similar with the LAA, the elements of the CAA are also assumed to be isotropic radiators. The AF of a CAA can be written as follows [4]:

$$\mathrm{AF}(\theta,\phi)=\sum_{i=1}^{N} I_n \exp\left(j\left[ka\sin(\theta)\cos(\phi-\phi_n)+\alpha_n\right]\right),$$
$$ka=\frac{2\pi}{\lambda}a=\sum_{i=1}^{N} d_i,$$
$$\phi_n=\frac{2\pi\sum_{i=1}^{n} d_i}{ka},$$
$$\alpha_n=-ka\sin(\theta_0)\cos(\phi_0-\phi_n), \tag{2}$$

where I_n is the excitation current of the nth element, α_n is the phase of the nth element, and d_n represents the arc distance between elements n and $n-1$ (d_1 is the arc distance between the first ($n=1$) and the last ($n=N$) elements). ϕ_n and θ_n represent the azimuth angle measured from the positive x-axis and the elevation angle measured from the z-axis, respectively. Moreover, θ_0 and ϕ_0 are set to be 90° and 0°, respectively.

3. Problem Formulation

This work is aiming to design the antenna arrays with minimum SLL. The excitation currents I of the antenna elements affect the beam pattern directly; hence, an optimal set of excitation currents for each element need to be determined to achieve lower SLL. Therefore, the optimization problem can be formulated as follows:

Minimize

$$f=10\log_{10}\frac{|\mathrm{AF}(\phi_{\mathrm{MSL}})|}{|\mathrm{AF}(\phi_{\mathrm{ML}})|}, \tag{3}$$

subject to

$$\phi_{\mathrm{ML}}=\arg\max|\mathrm{AF}(\phi)|, \quad \phi\in[-\pi,\pi], \tag{4}$$

$$\phi_{\mathrm{MSL}}\in\max([-\pi,\phi_{\mathrm{FN1}}]\cup[\phi_{\mathrm{FN2}},\pi]), \tag{5}$$

$$0\le I_n\le 1, \tag{6}$$

where ϕ_{MSL} is the angle of the maximum SLL and ϕ_{ML} is the angle of the mainlobe, ϕ_{FN1} and ϕ_{FN2} are the first nulls in $(-\pi, \phi_{\mathrm{FN1}})$ and $(-\pi, \phi_{\mathrm{FN2}})$, respectively, and the first null beamwidth (FNBW) of the beam pattern can be determined by them. The constraint (4) determines the location of the mainlobe, the constraint (5) shows the range of the sidelobe, and the constraint (6) specifies the range of the normalized excitation current of each element.

4. Invasive Weed Optimization Algorithm

IWO is a novel numerical stochastic optimization algorithm inspired from weed colonization, and it is first proposed by Mehrabian and Lucas in reference [24]. In the IWO approach, the whole population is composed of a certain number of weeds, and each weed is made up of a set of decision variables. The weed is a plant that is vigorous and invasive, and it poses a serious threat to the desirable plants. These features show that the weeds are very robust and troublous in the agriculture.

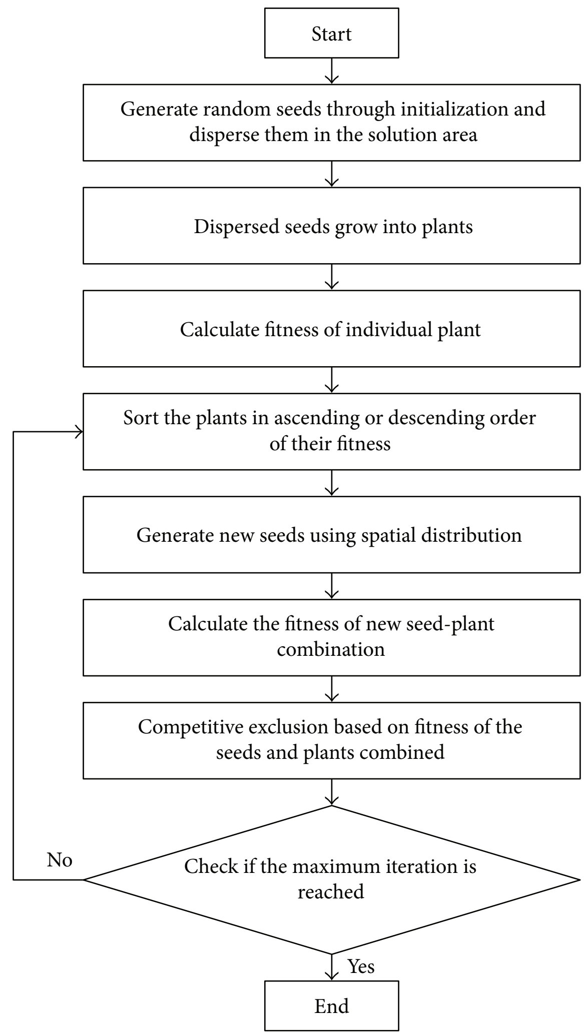

Figure 3: Flowchart of the IWO algorithm.

The working mechanism of IWO tried to imitate adaptation, robustness, and randomness of weeds in a very concise and efficient pattern. For a minimization problem, a weed with lower fitness value can generate more number of seeds. On the contrary, a weed with higher fitness value generates less number of seeds. The number of the newly generated seeds is decreased linearly from the maximum to the minimum allowable seeds in the colony. These newly generated seeds will be dispersed among the solution space with mean zero and varying standard deviations of normal distribution, and they will grow into new weeds. These weeds will generate new seeds. Moreover, in order to keep the certain number of the whole population, the weeds with worse fitness values will be eliminated from the colony.

The main procedure of IWO is shown in Figure 3, and the details of this algorithm are presented as follows.where $S_{\min}$ and $S_{\max}$ are the minimum and maximum number of the seeds, respectively, f is the fitness value of a certain weed, f_{worst} and f_{best} denote the worst and best fitness values in a certain iteration, respectively, and floor is the round down operation.where $\sigma_{\mathrm{initial}}$ and σ_{final} are the predefined initial and final standard deviations, respectively. iter is the current

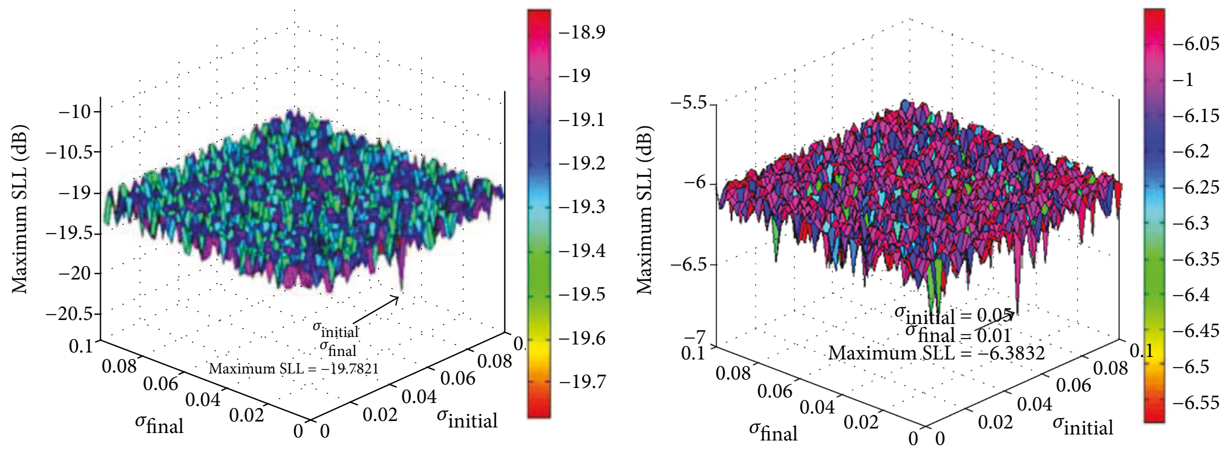

(a) (b)

Figure 4: Parameter tunings for σ_{initial} and σ_{final} in IWO for reducing the maximum SLL of the 8-element antenna arrays. (a) LAA. (b) CAA.

iteration and m is the nonlinear modulation index. W^{iter} is a weed in the iterth iteration, $N(0, \sigma_{\text{iter}}^2)$ is a normal random number with mean zero and standard deviation σ_{iter}.

Step 1. Initialization. In the first step of IWO, the algorithm initializes a certain number of weeds (candidate solutions) to construct a population and disperse these solutions to the d dimensional problem space uniformly and randomly.

Step 2. Reproduction. In this step, each solution in the population reproduces seeds according to its own lowest and highest fitness values in the colony. The number of seeds reproduced by a weed is given as follows:

$$S = \text{floor}\left[S_{\min} + (S_{\max} - S_{\min}) \times \frac{f - f_{\text{worst}}}{f_{\text{best}} - f_{\text{worst}}}\right], \quad (7)$$

Step 3. Spatial dispersal. Next, the newly generated seeds will be distributed over the d dimensional searching space and randomly spread in the vicinity of their parent weeds in the normal distribution with mean zero and varying standard deviations, to grow into new weeds. By this way, the search efficiency can be enhanced. The computing method of the standard deviation σ_{iter} in a specific iteration is shown in (8), and the new weeds can be generated by (9).

$$\sigma_{\text{iter}} = \frac{(\text{iter}_{\max} - \text{iter})^m}{\text{iter}_{\max}{}^m} \times (\sigma_{\text{initial}} - \sigma_{\text{final}}) + \sigma_{\text{final}}, \quad (8)$$

$$W_{\text{new}}^{\text{iter}} = W^{\text{iter}} + N(0, \sigma_{\text{iter}}^2), \quad (9)$$

Step 4. Competitive exclusion. After several iterations, the number of weeds in the colony will exceed the predefined maximum limited value due to the growth and reproduction of the weeds. Therefore, an elimination mechanism needs to be applied to eliminate the weeds with worse fitness values until the maximum number of weeds in the colony is reached. Then, the reserved ones will remain to the next iteration.

For the beam pattern synthesis of the antenna array with IWO, the excitation currents of the elements can be regarded as a candidate solution in IWO and the solution can be expressed as follows:

$$x = (I_1, I_2, I_3, \ldots, I_n), \quad (10)$$

where n is the number of antenna elements. Then, the population of IWO can be written as follows:

$$\text{pop} = \begin{bmatrix} x_1 \\ x_1 \\ \cdots \\ x_N \end{bmatrix} = \begin{bmatrix} I_1^1, I_2^1, I_3^1, \ldots, I_n^1 \\ I_1^2, I_2^2, I_3^2, \ldots, I_n^2 \\ \cdots \\ I_1^N, I_2^N, I_3^N, \ldots, I_n^N \end{bmatrix}, \quad (11)$$

where N is the population size.

5. Simulation and Analysis

In this section, the beam pattern synthesis for reducing the SLL of the LAA and the CAA is simulated by Matlab. The simulations are performed on a computer with an Intel (R) Core (TM) 2 Duo CPU and a 3.00 GB RAM. First, the main parameters of IWO are tuned to achieve the best performance for the beam pattern synthesis. Second, usage of IWO to synthesize the beam pattern is simulated and the results are compared with CS, FA, BBO, and PSO. Then, the stabilities of IWO and these benchmark algorithms are compared. Finally, we conduct EM simulations to verify the optimization performance of the antenna arrays in practical conditions.

5.1. Parameter Tunings and Setups. The parameter values of σ_{initial} and σ_{final} control the main updating procedure of IWO. Thus, they will be jointly tuned for achieving better performance of the algorithm. In the tuning test, the ranges of σ_{initial} and σ_{final} are (0.01, 0.1) and (0.01, 0.1), respectively, and the steps are both 0.002. Thus, the total number of points for a tuning test is 2500. The tests are independently repeated for 50 times and the average values are

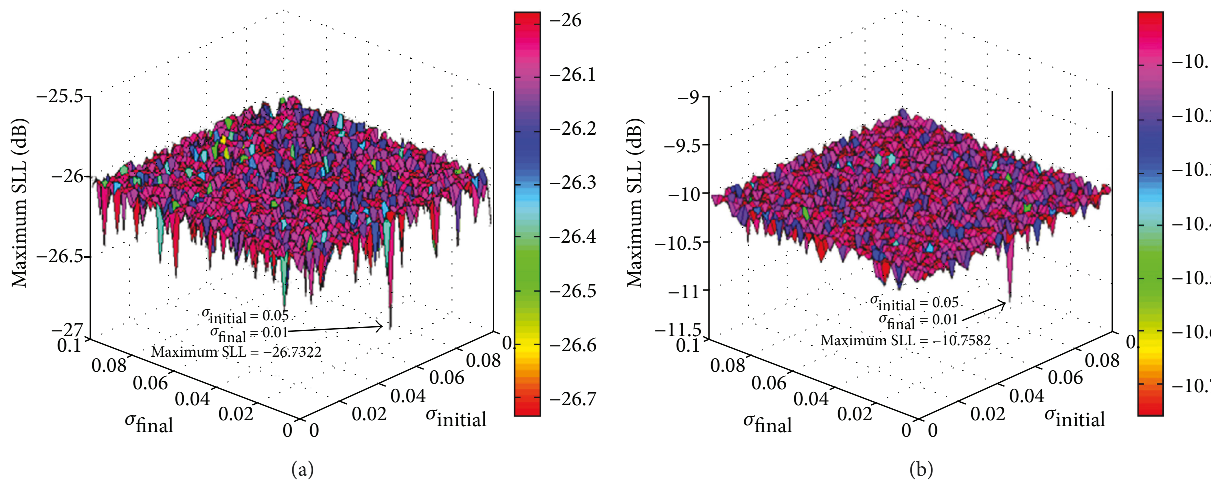

Figure 5: Parameter tunings for σ_{initial} and σ_{final} in IWO for reducing the maximum SLL of the 16-element antenna arrays. (a) LAA. (b) CAA.

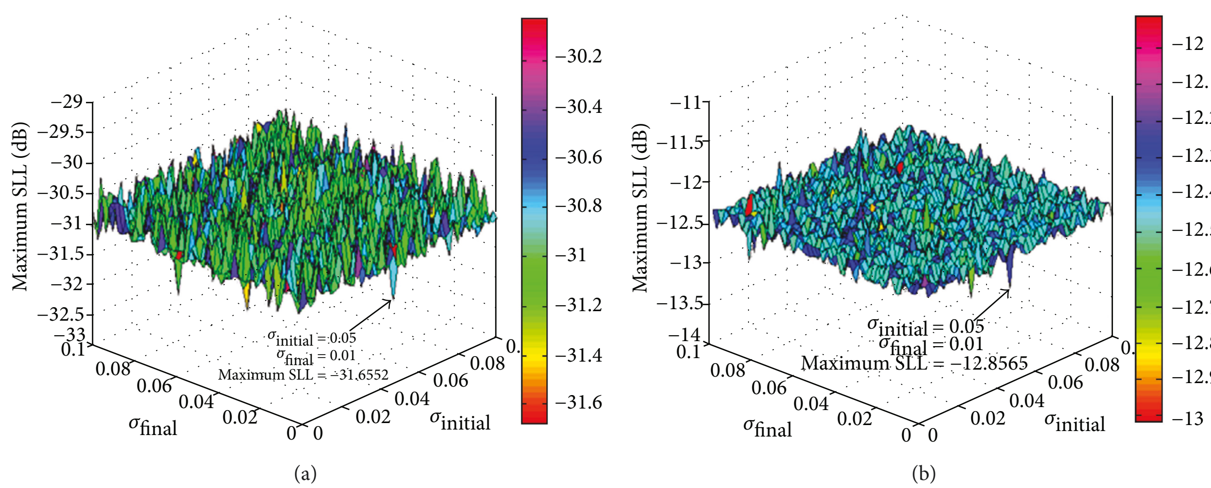

Figure 6: Parameter tunings for σ_{initial} and σ_{final} in IWO for reducing the maximum SLL of the 32-element antenna arrays. (a) LAA. (b) CAA.

Table 1: Parameter setups of IWO.

Parameters	Values
$S_{\max}$	5
$S_{\min}$	0
σ_{initial}	0.05
σ_{final}	0.01
m	3

presented. Figures 4(a), 4(b), 5(a), 5(b), 6(a), and 6(b) show the tuning results of the LAAs and the CAAs with 8, 16, and 32 elements. It can be seen from the figures that the optimal values of σ_{initial} and σ_{final} are 0.05 and 0.01, respectively, for both LAA and CAA.

The other parameters of IWO and the benchmark algorithms are shown in Table 1. Moreover, for the benchmark algorithms, we use the versions and the parameter values in [26–29] for BBO, CS, FA, and PSO, and the detailed parameter setups of these algorithms are shown in Table 2. Moreover, the population size and the maximum iteration of each algorithm are 20 and 200, respectively, for fairness.

Table 2: Parameter setups of the benchmark algorithms.

Algorithms	Parameters
BBO	Habitat modification probability: 1; immigration rate: 1; emigration rate: 1; mutation rate: 0.005
CS	Probability of egg detection: 0.25; step size of Lévy flight: 1
FA	Light absorption coefficient: 0.2; step factor: 0.6
PSO	Learning factor 1: 2; learning factor 2: 2

The time complexities of the algorithms above are analyzed here. The main computational cost will be the fitness function evaluations. Supposing the maximum number of iteration is t for each algorithm, then the time complexity of IWO is $O(N \cdot t)$ because there is only one inner loop in the algorithm; N is the population size. CS, FA, BBO, and PSO have similar algorithm structure with IWO; hence, the time complexities of these benchmark algorithms are also $O(N \cdot t)$. As can be seen, the computational costs of these algorithms are relatively inexpensive because the complexities are linear in terms of t.

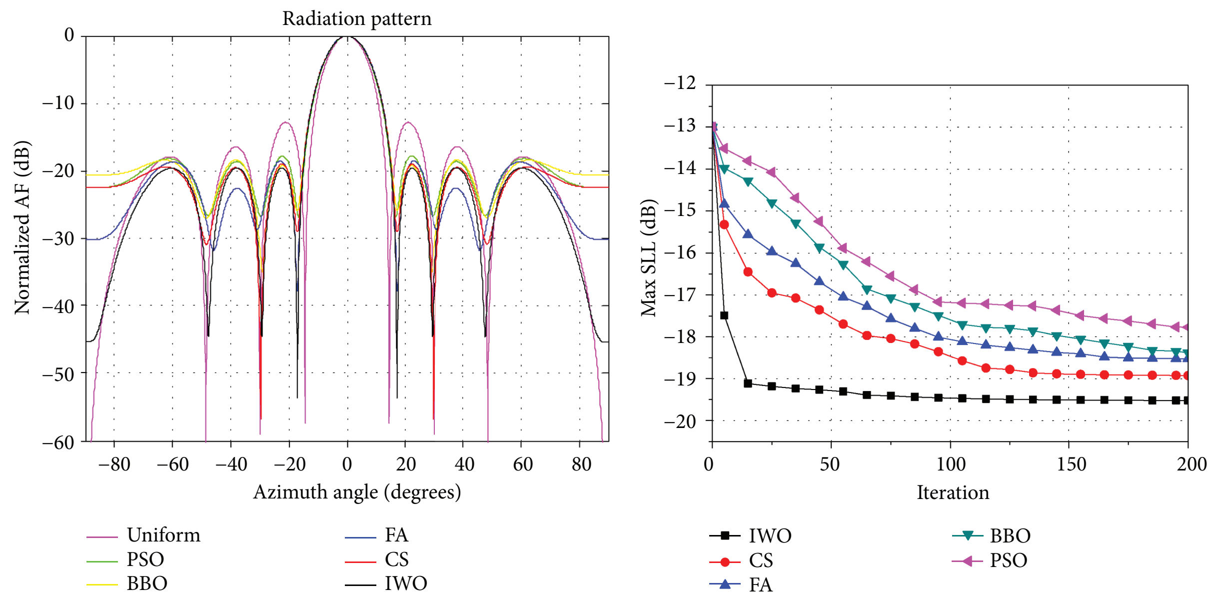

(a) (b)

Figure 7: Beam patterns and convergence rates of the 8-element LAA obtained by different algorithms. (a) Beam patterns. (b) Convergence rates.

Table 3: Excitation currents and maximum SLL of the 8-element LAA obtained by different algorithms.

Algorithm	$(I_1, I_2, I_3, I_4, I_5, I_6, I_7, I_8)$	Max SLL (dB)
IWO	0.5891, 0.6562, 0.8840, 0.9855, 1.0000, 0.8575, 0.6712, 0.6115	−19.5215
CS	0.5853, 0.5491, 0.8083, 0.8071, 0.7859, 0.6131, 0.5531, 0.3801	−18.9278
FA	0.7033, 0.7033, 0.9412, 0.9381, 0.9565, 0.9082, 0.5943, 0.4540	−18.5229
BBO	0.4311, 0.4227, 0.6133, 0.6035, 0.8779, 0.6096, 0.5785, 0.4397	−18.3868
PSO	0.4634, 0.6319, 0.8124, 1.0000, 1.0000, 1.0000, 0.7746, 0.9151	−17.7736
Uniform	1.0000, 1.0000, 1.0000, 1.0000, 1.0000, 1.0000, 1.0000, 1.0000	−12.7972

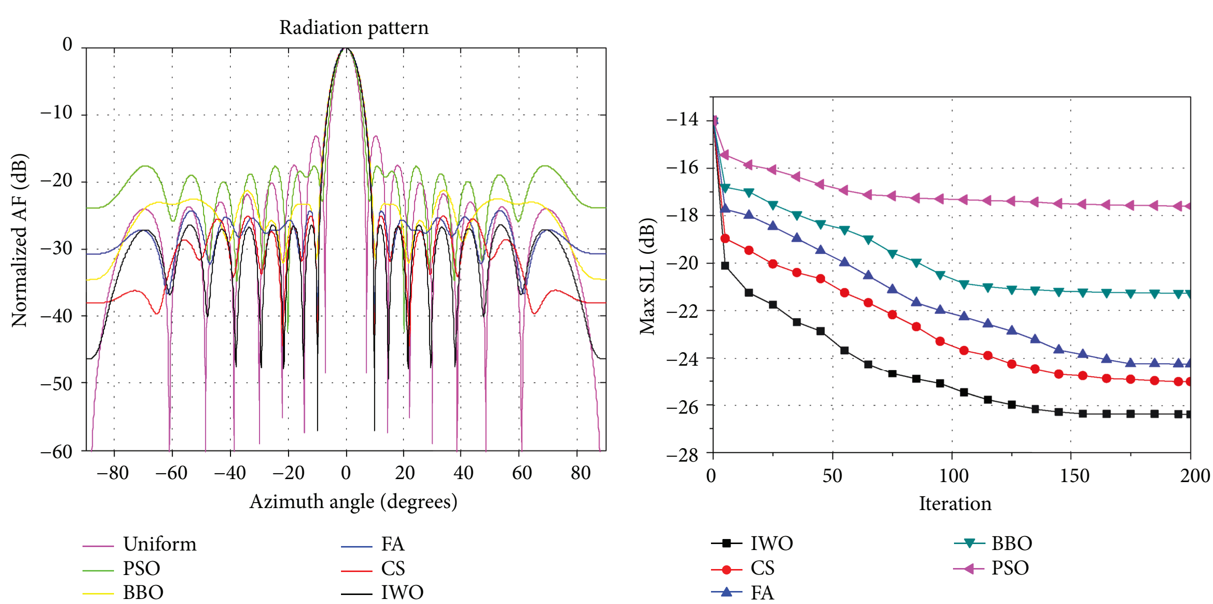

(a) (b)

Figure 8: Beam patterns and convergence rates of the 16-element LAA obtained by different algorithms. (a) Beam patterns. (b) Convergence rates.

Table 4: Excitation currents and maximum SLL of the 16-element LAA obtained by different algorithms.

Algorithm	$(I_1, I_2, I_3, I_4, I_5, I_6, I_7, I_8, I_9, I_{10}, I_{11}, I_{12}, I_{13}, I_{14}, I_{15}, I_{16})$	Max SLL (dB)
IWO	0.3816, 0.3518, 0.4807, 0.5730, 0.7230, 0.8449, 0.8716, 0.9607, 0.9015, 0.9152, 0.8064, 0.7165, 0.6284, 0.4646, 0.3593, 0.3754	−26.3889
CS	0.2746, 0.4124, 0.4454, 0.6572, 0.6341, 0.7431, 0.8423, 0.8115, 0.9066, 0.7848, 0.7173, 0.7259, 0.5137, 0.3320, 0.3200, 0.3043	−25.0106
FA	0.2945, 0.3581, 0.4739, 0.6472, 0.6065, 0.6275, 0.7910, 0.9785, 0.7978, 0.6976, 0.7821, 0.6515, 0.5205, 0.4430, 0.1535, 0.2805	−24.2705
BBO	0.2211, 0.1887, 0.3124, 0.2465, 0.7824, 0.6565, 0.7495, 0.8711, 0.8811, 1.0000, 0.5846, 0.8090, 0.8059, 0.5463, 0.5439, 0.3832	−21.2792
PSO	1.0000, 0.0131, 0.4806, 0.5739, 1.0000, 1.0000, 1.0000, 1.0000, 1.0000, 1.0000, 1.0000, 1.0000, 1.0000, 1.0000, 1.0000, 1.0000	−17.6110
Uniform	1.0000, 1.0000, 1.0000, 1.0000, 1.0000, 1.0000, 1.0000, 1.0000, 1.0000, 1.0000, 1.0000, 1.0000, 1.0000, 1.0000, 1.0000, 1.0000	−13.1476

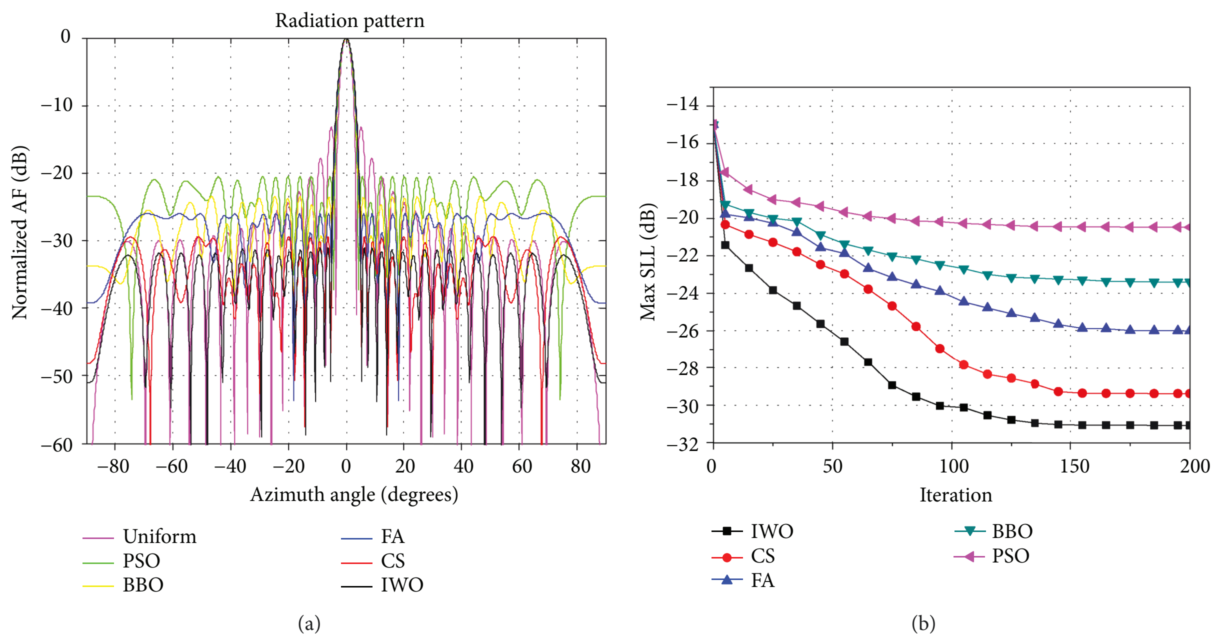

Figure 9: Beam patterns and convergence rates of the 32-element LAA obtained by different algorithms. (a) Beam patterns. (b) Convergence rates.

5.2. Beam Pattern Synthesis of the LAA. In this section, we use different algorithms to synthesize the beam patterns of the 8-element, 16-element, and 32-element LAAs, to compare the performances of these algorithms for the different dimensions of solutions.

5.2.1. Sample 1: Beam Pattern Synthesis for the 8-Element LAA. Figure 7(a) shows the beam patterns of an 8-element LAA obtained by the uniform array, PSO, BBO, FA, CS, and IWO. Note that the uniform array means that the excitation current of each antenna element is fixed as 1. Figure 7(b) shows the convergence rates during the optimization process of different algorithms. As can be seen, IWO has the best performance in terms of the accuracy as well as the convergence rate. Table 3 shows the maximum SLL obtained by these methods. It can be seen that the maximum SLL obtained by IWO is −19.5215 dB, which is the lowest among all the algorithms. Moreover, the excitation currents optimized by each algorithm is also listed in Table 3.

5.2.2. Sample 2: Beam Pattern Synthesis for the 16-Element LAA. In this sample, the beam patterns of a LAA with 16 elements are synthesized by different approaches. Figure 8(a) shows the beam patterns obtained by different algorithms and Figure 8(b) shows the convergence rate of these algorithms. Table 4 compares the numerical results. It can be seen from the figures and table that IWO has the best performance in terms of the maximum SLL suppression and convergence rate in this case. In addition, the excitation currents obtained by different algorithms are also shown in Table 4.

5.2.3. Sample 3: Beam Pattern Synthesis for the 32-Element LAA. Figure 9(a) shows the beam patterns of a 32-element LAA optimized by different algorithms, and Table 5 presents that the maximum SLLs obtained by IWO, CS, FA,

Table 5: Excitation currents and maximum SLL of the 32-element LAA obtained by different algorithms.

Algorithm	$(I_1, I_2, I_3, I_4, I_5, I_6, I_7, I_8, I_9, I_{10}, I_{11}, I_{12}, I_{13}, I_{14}, I_{15}, I_{16}, I_{17}, I_{18}, I_{19}, I_{20}, I_{21}, I_{22}, I_{23}, I_{24}, I_{25}, I_{26}, I_{27}, I_{28}, I_{29}, I_{30}, I_{31}, I_{32})$	Max SLL (dB)
IWO	0.3595, 0.2528, 0.2958, 0.3072, 0.3827, 0.5186, 0.5869, 0.6160, 0.7092, 0.7786, 0.8304, 0.8904, 0.9424, 0.9575, 1.0000, 0.9988, 0.9969, 1.0000, 0.9757, 0.9049, 0.8868, 0.8317, 0.7572, 0.7039, 0.6628, 0.5290, 0.4582, 0.4497, 0.3931, 0.2831, 0.1987, 0.3559	−31.0751
CS	0.2486, 0.2294, 0.2216, 0.2620, 0.3370, 0.3843, 0.5987, 0.4521, 0.6567, 0.7068, 0.6782, 0.8299, 0.7822, 0.8434, 0.9187, 0.8264, 0.8709, 0.9340, 0.8826, 0.9019, 0.7806, 0.7302, 0.6980, 0.6499, 0.6384, 0.4761, 0.4184, 0.4811, 0.3425, 0.3564, 0.2256, 0.3078	−29.3774
FA	0.3088, 0.3535, 0.2421, 0.2778, 0.2115, 0.5247, 0.5540, 0.5362, 0.6946, 0.4153, 0.9206, 0.7328, 0.7733, 0.6621, 0.8531, 0.9776, 0.6737, 0.8532, 0.8282, 0.6933, 0.6005, 0.7362, 0.4963, 0.7293, 0.4923, 0.3749, 0.4827, 0.4852, 0.2467, 0.4119, 0.3348, 0.1415	−26.0192
BBO	0.5337, 0.4577, 0.2699, 0.3218, 0.5073, 0.5301, 0.7161, 0.4816, 0.8820, 0.7761, 0.7917, 0.8377, 0.6430, 1.0000, 0.9200, 0.7889, 0.9439, 1.0000, 0.9507, 0.9818, 0.8549, 0.9857, 0.6930, 0.7569, 0.7569, 0.6903, 0.1542, 0.2614, 0.6717, 0.2748, 0.4760, 0.1863	−23.4108
PSO	0.4101, 1.0000, 1.0000, 0.1596, 0.5696, 1.0000, 1.0000, 0.4572, 1.0000, 0.8231, 1.0000, 1.0000, 1.0000, 1.0000, 1.0000, 1.0000, 1.0000, 1.0000, 1.0000, 1.0000, 0.8257, 1.0000, 1.0000, 0.9728, 0.5698, 1.0000, 0.2918, 0.0373, 0.9013, 0.0004, 1.0000, 0.4027	−20.4785
Uniform	1.0000, 1.0000	−13.2318

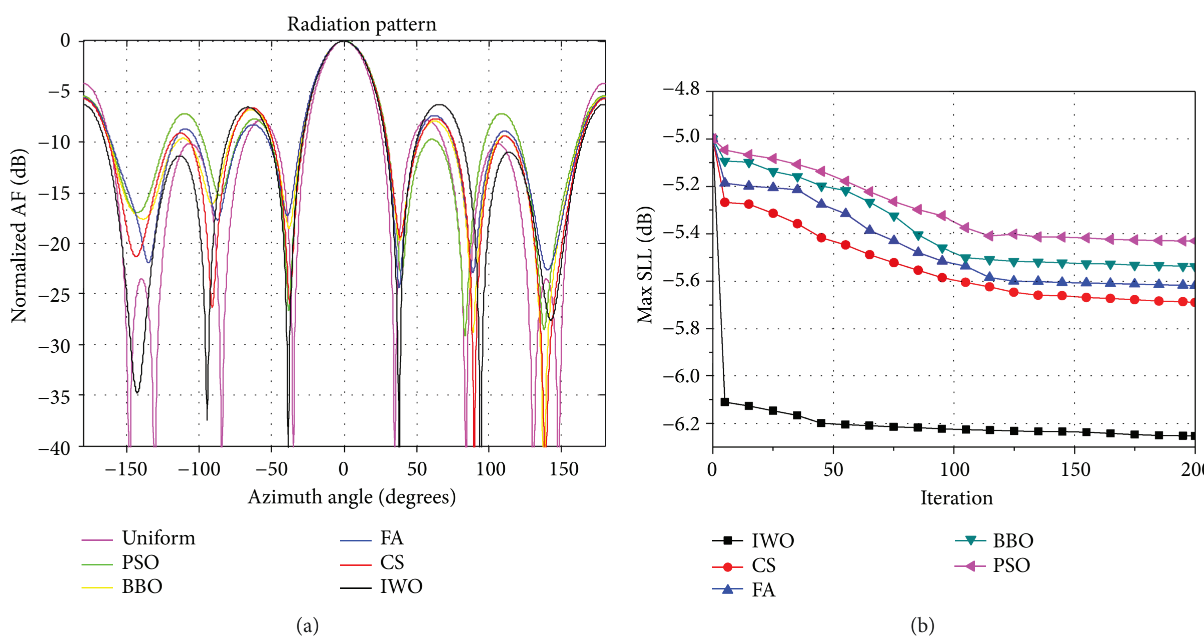

Figure 10: Beam patterns and convergence rates of the 8-element CAA obtained by different algorithms. (a) Beam patterns. (b) Convergence rates.

Table 6: Excitation currents and maximum SLLs of the 8-element CAA obtained by different algorithms.

Algorithm	$(I_1, I_2, I_3, I_4, I_5, I_6, I_7, I_8)$	Max SLL (dB)
IWO	0.3985, 0.6434, 0.4675, 1.0000, 0.4329, 0.6780, 0.4401, 0.9638	**−6.2535**
CS	0.8433, 0.5502, 0.3853, 0.9240, 0.2821, 0.5422, 0.4995, 0.8207	−5.6903
FA	0.5079, 0.8003, 0.6064, 0.6958, 0.4866, 0.2004, 0.5056, 0.9449	−5.6191
BBO	0.2853, 0.2541, 0.5133, 0.7834, 0.6841, 0.7279, 0.3247, 0.6775	−5.5380
PSO	0.9702, 1.0000, 0.4337, 1.0000, 0.7317, 0.0000, 1.0000, 1.0000	−5.4304
Uniform	1.0000, 1.0000, 1.0000, 1.0000, 1.0000, 1.0000, 1.0000, 1.0000	−4.1702

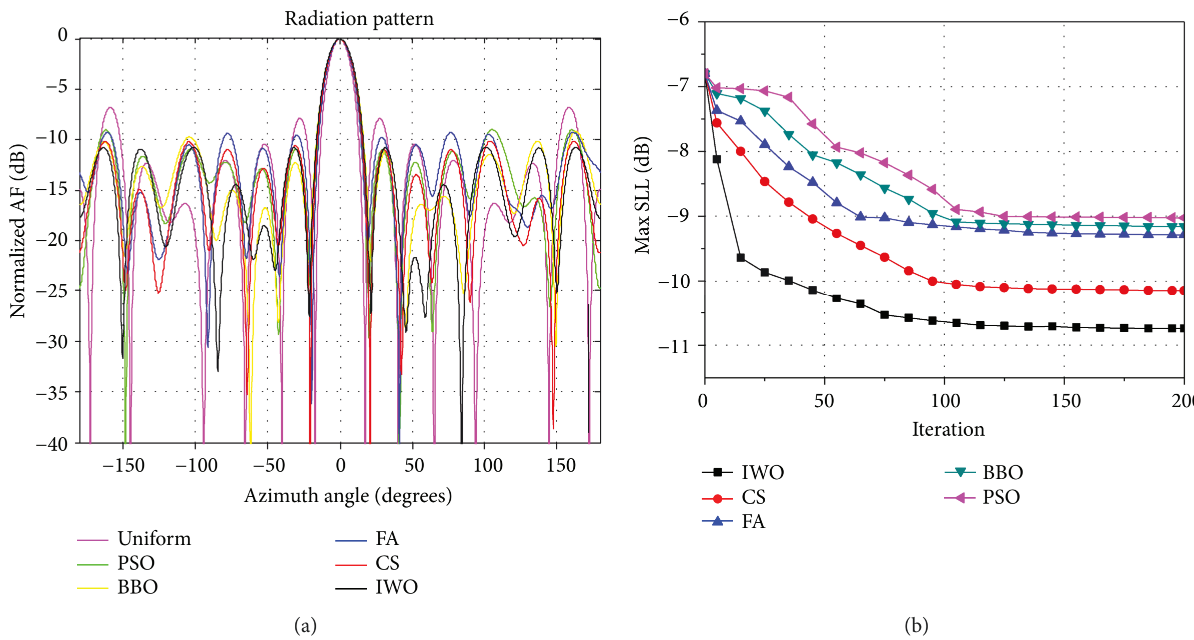

FIGURE 11: Beam patterns and convergence rates of the 16-element CAA obtained by different algorithms. (a) Beam patterns. (b) Convergence rates.

TABLE 7: Excitation currents and maximum SLLs of the 16-element CAA obtained by different algorithms.

Algorithm	$(I_1, I_2, I_3, I_4, I_5, I_6, I_7, I_8, I_9, I_{10}, I_{11}, I_{12}, I_{13}, I_{14}, I_{15}, I_{16})$	Max SLL (dB)
IWO	0.6134, 0.8125, 0.1244, 0.0000, 0.2476, 0.8644, 0.6049, 0.8260, 0.3362, 0.9878, 0.1337, 0.0000, 0.0091, 0.9322, 0.3423, 0.6827	−10.7440
CS	0.5780, 0.7596, 0.2491, 0.0546, 0.1192, 0.7774, 0.7137, 0.4641, 0.7711, 0.6402, 0.2849, 0.0799, 0.4616, 0.5811, 0.6121, 0.7003	−10.1490
FA	0.3282, 0.8088, 0.3292, 0.2406, 0.3882, 0.4132, 0.8062, 0.4230, 0.8580, 0.2449, 0.2122, 0.2156, 0.2339, 0.6581, 0.3901, 0.4245	−9.2885
BBO	1.0000, 1.0000, 0.4136, 0.0000, 0.0000, 0.9361, 0.7941, 1.0000, 0.3357, 1.0000, 0.0000, 0.4629, 0.0000, 1.0000, 0.5478, 1.0000	−9.1592
PSO	1.0000, 1.0000, 0.2790, 0.0003, 1.0000, 1.0000, 1.0000, 1.0000, 0.7687, 0.9998, 0.0000, 1.0000, 0.0000, 0.9998, 0.9564, 1.0000	−9.0261
Uniform	1.0000, 1.0000, 1.0000, 1.0000, 1.0000, 1.0000, 1.0000, 1.0000, 1.0000, 1.0000, 1.0000, 1.0000, 1.0000, 1.0000, 1.0000, 1.0000	−6.7578

BBO, and PSO are −31.0751 dB, −29.3774 dB, −26.0192 dB, −23.4108 dB, and −20.4785 dB, respectively. Moreover, the maximum SLL of the uniform array is −13.2318 dB. The excitation currents of these algorithms are also presented in the table. Figure 9(b) shows the convergence rates during the optimization process. Similar to the previous samples, IWO also has the best performance for this case.

5.3. Beam Pattern Synthesis of the CAA. The beam pattern synthesis results of the CAA are presented in this section. Corresponding to the case of LAA, three samples that are 8-element, 16-element, and 32-element CAAs are optimized by different algorithms.

5.3.1. Sample 4: Beam Pattern Synthesis for the 8-Element CAA. Figure 10(a) shows the beam patterns of an 8-element CAA optimized by different algorithms, and the convergence rates of these methods are shown in Figure 10(b). The maximum SLLs obtained by these algorithms are listed in Table 6. As can be seen, the maximum SLL obtained by IWO is −6.2535 dB, which is the lowest among all the approaches. Moreover, the excitation currents obtained by different algorithms are also shown in Table 6.

5.3.2. Sample 5: Beam Pattern Synthesis for the 16-Element CAA. In this sample, we use different algorithms to optimize a 16-element CAA. Figures 11(a) and 11(b) show the beam pattern results and the convergence rates, respectively, and Table 7 compares the numerical results of the maximum SLL. As can be seen, the maximum SLL obtained by the uniform array, CS, FA, BBO, and PSO are −6.7578 dB, −10.1490 dB, −9.2885 dB, −9.1592 dB, and −9.0261 dB, respectively, and it is −10.7440 dB by using IWO. Thus, IWO achieves the best results for reducing the maximum SLL. Moreover,

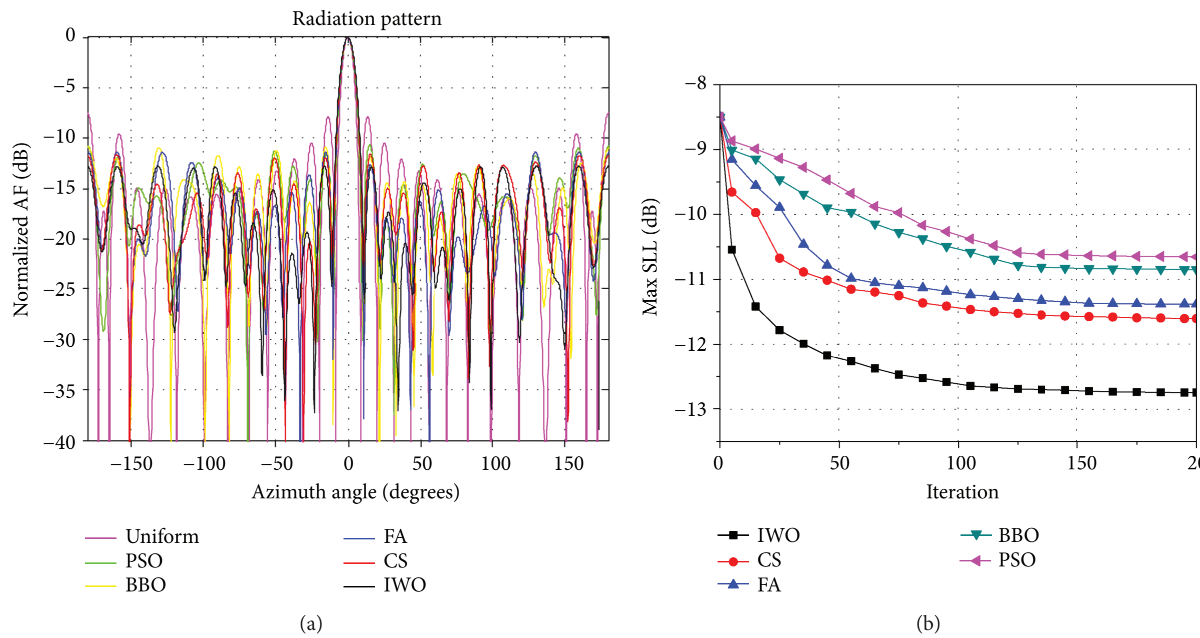

FIGURE 12: Beam patterns and convergence rates of the 32-element CAA obtained by different algorithms. (a) Beam patterns. (b) Convergence rates.

TABLE 8: Excitation currents and maximum SLL of the 32-element CAA obtained by different algorithms.

Algorithm	$(I_1, I_2, I_3, I_4, I_5, I_6, I_7, I_8, I_9, I_{10}, I_{11}, I_{12}, I_{13}, I_{14}, I_{15}, I_{16}, I_{17}, I_{18}, I_{19}, I_{20}, I_{21}, I_{22}, I_{23}, I_{24}, I_{25}, I_{26}, I_{27}, I_{28}, I_{29}, I_{30}, I_{31}, I_{32})$	Max SLL (dB)
IWO	0.6962, 0.8724, 0.9469, 0.3662, 0.6728, 0.0000, 0.1661, 0.1986, 0.3027, 0.0027, 0.4057, 0.4835, 0.8900, 0.9488, 0.5514, 0.3984, 0.6691, 0.9885, 0.5369, 0.5013, 0.1124, 0.0000, 0.2475, 0.5433, 0.0866, 0.0022, 0.2773, 0.4401, 0.5761, 0.9800, 0.6543, 0.6568	−12.7489
CS	0.4882, 0.7702, 0.6405, 0.3620, 0.6630, 0.0012, 0.0000, 0.4578, 0.6467, 0.0000, 0.6134, 0.9036, 1.0000, 1.0000, 0.3819, 0.7429, 1.0000, 0.5358, 0.7066, 0.6653, 0.4260, 0.0733, 0.3589, 0.2861, 0.0822, 0.0613, 0.2267, 0.3179, 0.5606, 0.7464, 0.4997, 0.7752	−11.6105
FA	0.5033, 0.9810, 0.9763, 0.7815, 0.2773, 0.2609, 0.2942, 0.2791, 0.3200, 0.4224, 0.1447, 0.5089, 0.4782, 0.4259, 0.9683, 0.6367, 0.8785, 0.7848, 0.5544, 0.8588, 0.3806, 0.1826, 0.1038, 0.3516, 0.3241, 0.0781, 0.4653, 0.4521, 0.7865, 0.9838, 0.6276, 0.5940	−11.3841
BBO	0.9960, 0.8963, 0.7448, 0.8392, 0.6942, 0.3150, 0.0000, 0.2426, 0.0171, 0.2492, 1.0000, 0.6806, 0.6796, 0.4954, 0.4173, 0.9256, 0.9525, 0.5485, 1.0000, 0.6544, 0.8278, 0.1468, 0.6944, 0.4708, 0.0000, 0.0000, 0.2895, 0.5924, 0.9188, 0.9119, 0.6243, 1.0000	−10.8523
PSO	0.4045, 1.0000, 1.0000, 0.6247, 1.0000, 0.0000, 0.0000, 0.9881, 1.0000, 0.0000, 0.0606, 0.8151, 1.0000, 1.0000, 0.6900, 0.4287, 1.0000, 0.6354, 0.6957, 1.0000, 0.0136, 0.0000, 1.0000, 0.3149, 0.0000, 0.3271, 0.6709, 0.3145, 1.0000, 1.0000, 0.8568, 1.0000	−10.6564
Uniform	1.0000, 1.0000	−7.5386

the excitation currents optimized by these algorithms are presented in Table 7.

5.3.3. Sample 6: Beam Pattern Synthesis for the 32-Element CAA. Figure 12(a) shows the beam patterns of a 32-element CAA optimized by different approaches, and the convergence rates of these algorithms are shown in Figure 12(b). Table 8 lists the maximum SLLs as well as the excitation currents obtained by these algorithms. Similar with the 8-element and the 16-element cases, IWO achieves the lowest SLL compared with other algorithms.

5.4. Stability Test. The swarm intelligence optimization algorithms such as PSO are stochastic, hence the optimization results that are likely to be different for each independent run. Therefore, statistical tests are necessary to analyze the performance of such algorithms. Thus, tests for synthesizing the beam patterns of the LAAs and the CAAs with different numbers of elements are conducted, and each test is with 30 independent trials.

Figures 13(a), 13(b), 14(a), 14(b), 15(a), and 15(b) show the maximum SLLs obtained by different algorithms of the 30 trials for the LAAs and the CAAs with different numbers

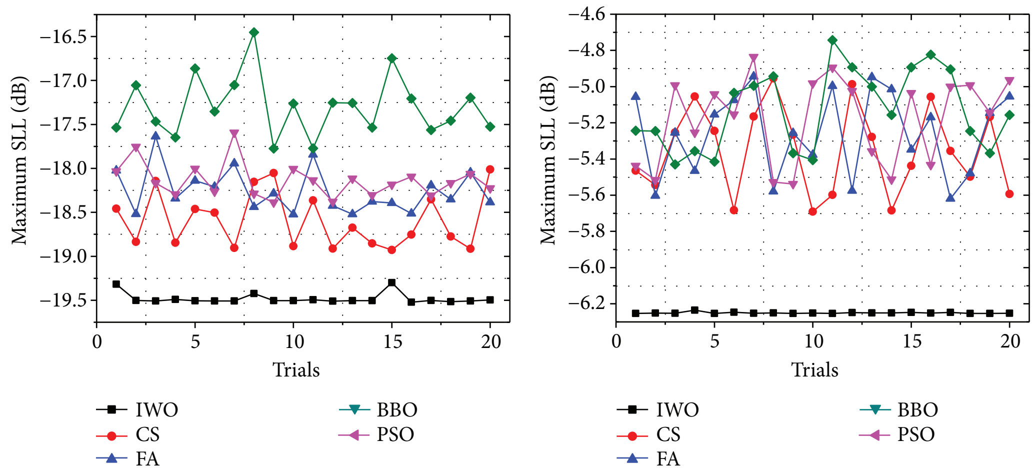

(a) (b)

Figure 13: Stability test results of different algorithms of the 8-element antenna arrays. (a) LAA. (b) CAA.

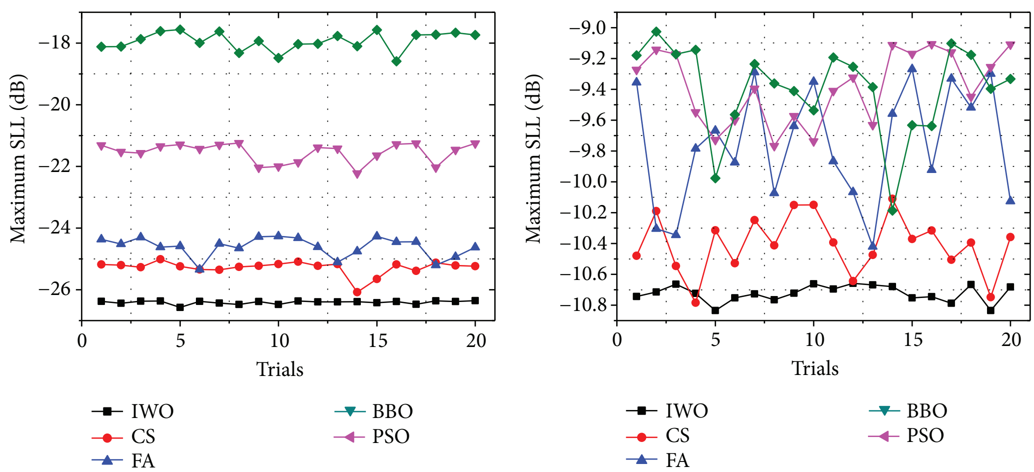

(a) (b)

Figure 14: Stability test results of different algorithms of the 16-element antenna arrays. (a) LAA. (b) CAA.

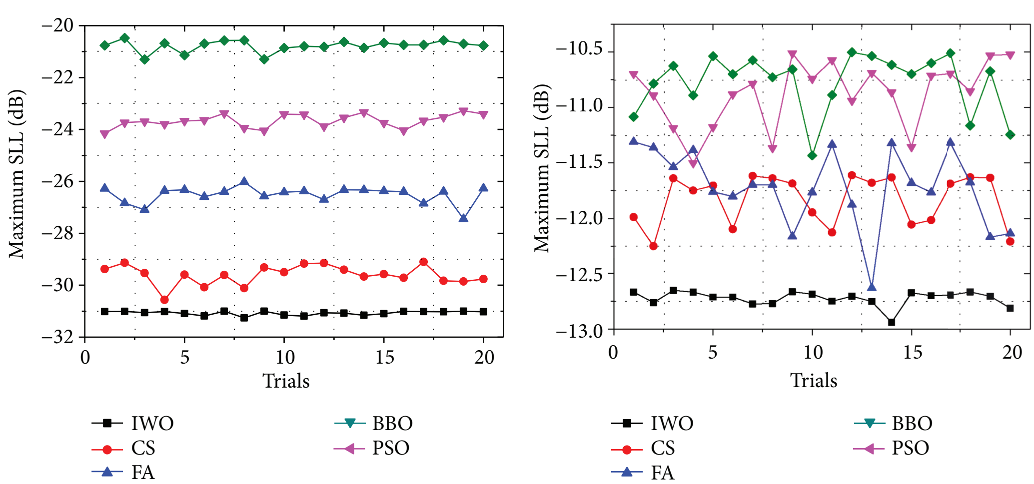

(a) (b)

Figure 15: Stability test results of different algorithms of the 32-element antenna arrays. (a) LAA. (b) CAA.

Table 9: Statistical results of different algorithms for the beam pattern synthesis of the 8-element LAA.

	IWO	CS	FA	BBO	PSO
Best max SLL (dB)	−19.5215	−18.9278	−18.5229	−18.3868	−17.7736
Worst max SLL (dB)	−19.2991	−18.0124	−17.6362	−17.5935	−16.4526
Mean max SLL (dB)	−19.4814	−18.5891	−18.2556	−18.1386	−17.2987
SD max SLL (dB)	0.0623	0.3190	0.2489	0.2489	0.3416

Table 10: Statistical results of different algorithms for the beam pattern synthesis of the 16-element LAA.

	IWO	CS	FA	BBO	PSO
Best max SLL (dB)	−26.5733	−26.0809	−25.3447	−22.2250	−18.5918
Worst max SLL (dB)	−25.3512	−25.0106	−24.2640	−21.2444	−17.5628
Mean max SLL (dB)	−26.4087	−25.2805	−24.6071	−21.5447	−17.9288
SD max SLL (dB)	0.0550	0.2293	0.3180	0.3140	0.2986

Table 11: Statistical results of different algorithms for the beam pattern synthesis of the 32-element LAA.

	IWO	CS	FA	BBO	PSO
Best max SLL (dB)	−31.2566	−30.5608	−27.4520	−24.1520	−21.3014
Worst max SLL (dB)	−31.0004	−29.1010	−26.0192	−23.2783	−20.4785
Mean max SLL (dB)	−31.0725	−29.6016	−26.5173	−23.6655	−20.7816
SD max SLL (dB)	0.0770	0.3706	0.3293	0.2554	0.2256

Table 12: Statistical results of different algorithms for the beam pattern synthesis of the 8-element CAA.

	IWO	CS	FA	BBO	PSO
Best max SLL (dB)	−6.2535	−5.6903	−5.6191	−5.5380	−5.4304
Worst max SLL (dB)	−6.2351	−4.9543	−4.9435	−4.8355	−4.7435
Mean max SLL (dB)	−6.2502	−5.3487	−5.2555	−5.1819	−5.1311
SD max SLL (dB)	0.0042	0.2408	0.2336	0.2399	0.2222

Table 13: Statistical results of different algorithms for the beam pattern synthesis of the 16-element CAA.

	IWO	CS	FA	BBO	PSO
Best max SLL (dB)	−10.8352	−10.7847	−10.4207	−9.7679	−10.1871
Worst max SLL (dB)	−10.6590	−10.1100	−9.2688	−9.1071	−9.0261
Mean max SLL (dB)	−10.7242	−10.4058	−9.7527	−9.3833	−9.3953
SD max SLL (dB)	0.0541	0.1895	0.3816	0.2323	0.2946

Table 14: Statistical results of different algorithms for the beam pattern synthesis of the 32-element CAA.

	IWO	CS	FA	BBO	PSO
Best max SLL (dB)	−12.9380	−11.2514	−12.6309	−11.5015	−11.4336
Worst max SLL (dB)	−12.6506	−11.6105	−11.3092	−10.5104	−10.5015
Mean max SLL (dB)	−12.7218	−11.8298	−11.7194	−10.8731	−10.7724
SD max SLL (dB)	0.0675	0.2268	0.3515	0.2972	0.2660

of antenna elements. Tables 9, 10, 11, 12, 13, and 14 show the statistical results in terms of the best, the worst, the mean values of the maximum SLLs, and the standard divisions (SD) of these trials. As can be seen, IWO achieves the lowest average maximum SLLs for both LAA and CAA. Moreover, the SDs of IWO are also the lowest which means that the

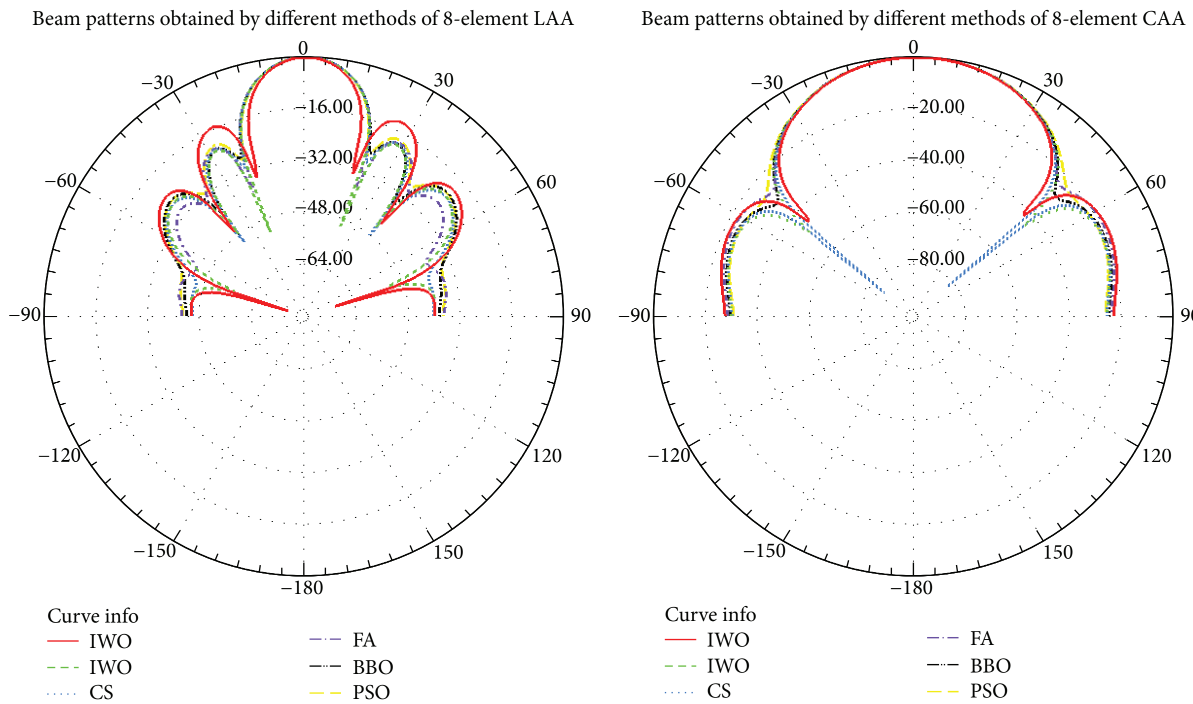

(a) (b)

Figure 16: 2D beam pattern comparisons in polar coordinates based on different excitation currents obtained by different optimization methods in EM simulations. (a) 8-element LAA. (b) 8-element CAA.

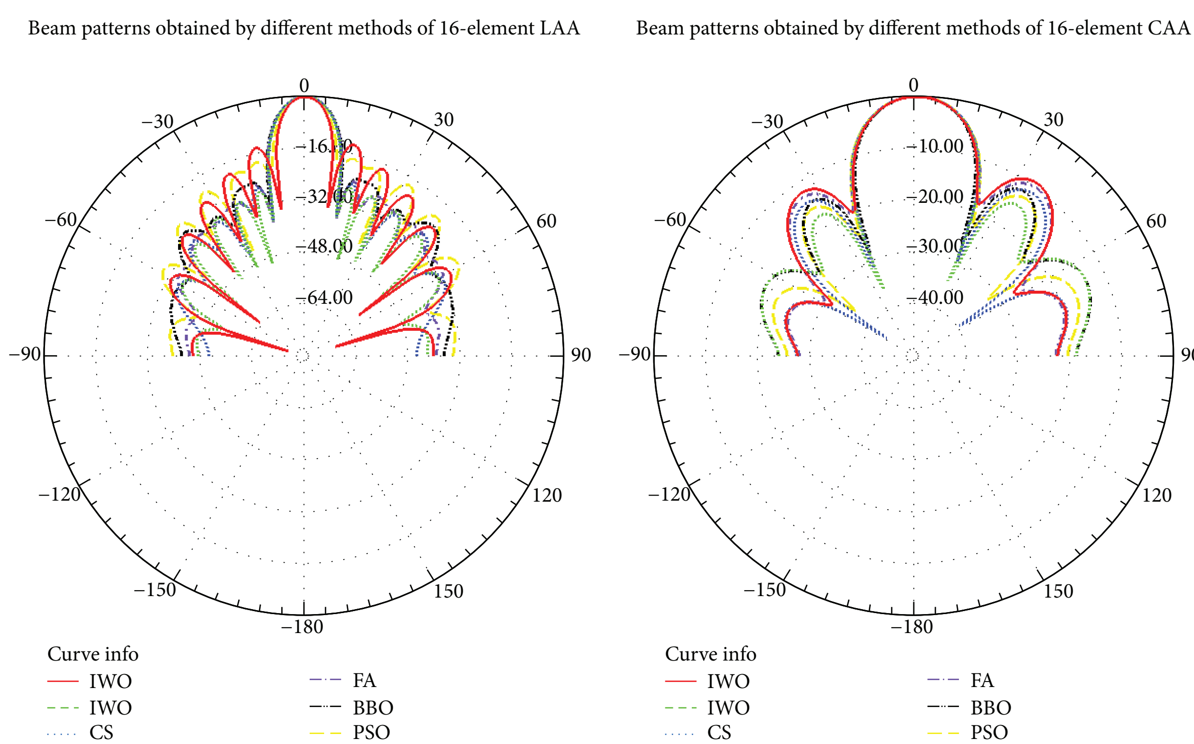

(a) (b)

Figure 17: 2D beam pattern comparisons in polar coordinates based on different excitation currents obtained by different optimization methods in EM simulations. (a) 16-element LAA. (b) 16-element CAA.

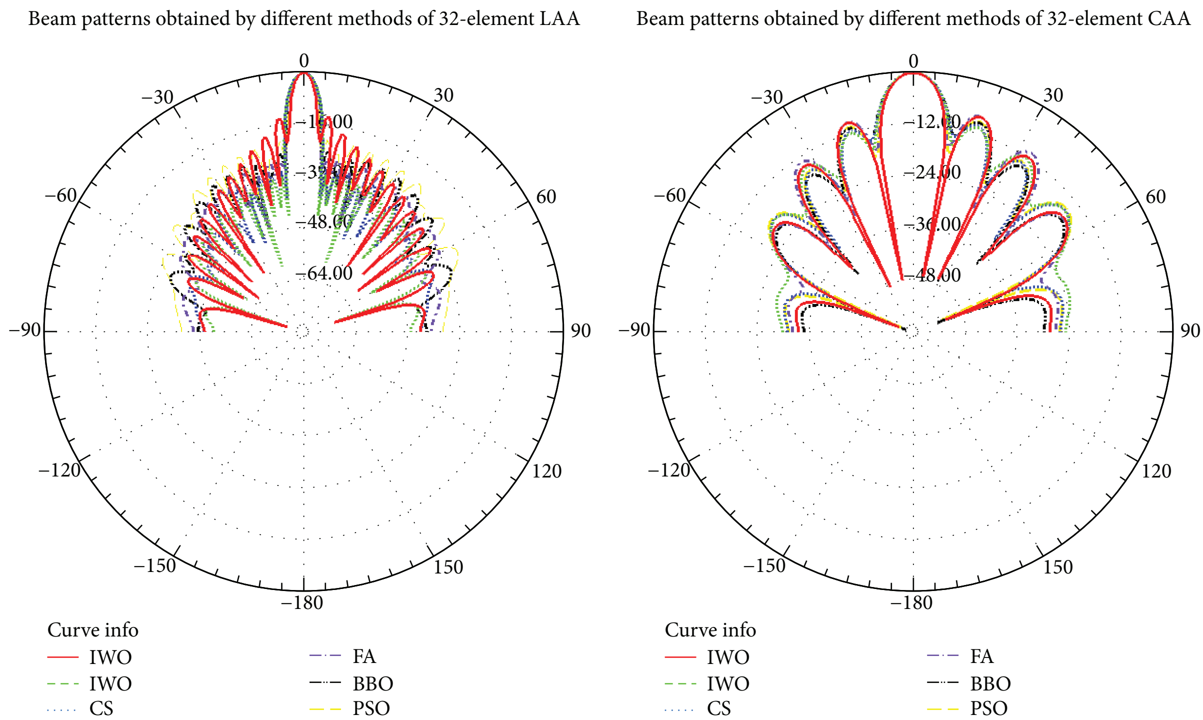

(a) (b)

Figure 18: 2D beam pattern comparisons in polar coordinates based on different excitation currents obtained by different optimization methods in EM simulations. (a) 32-element LAA. (b) 32-element CAA.

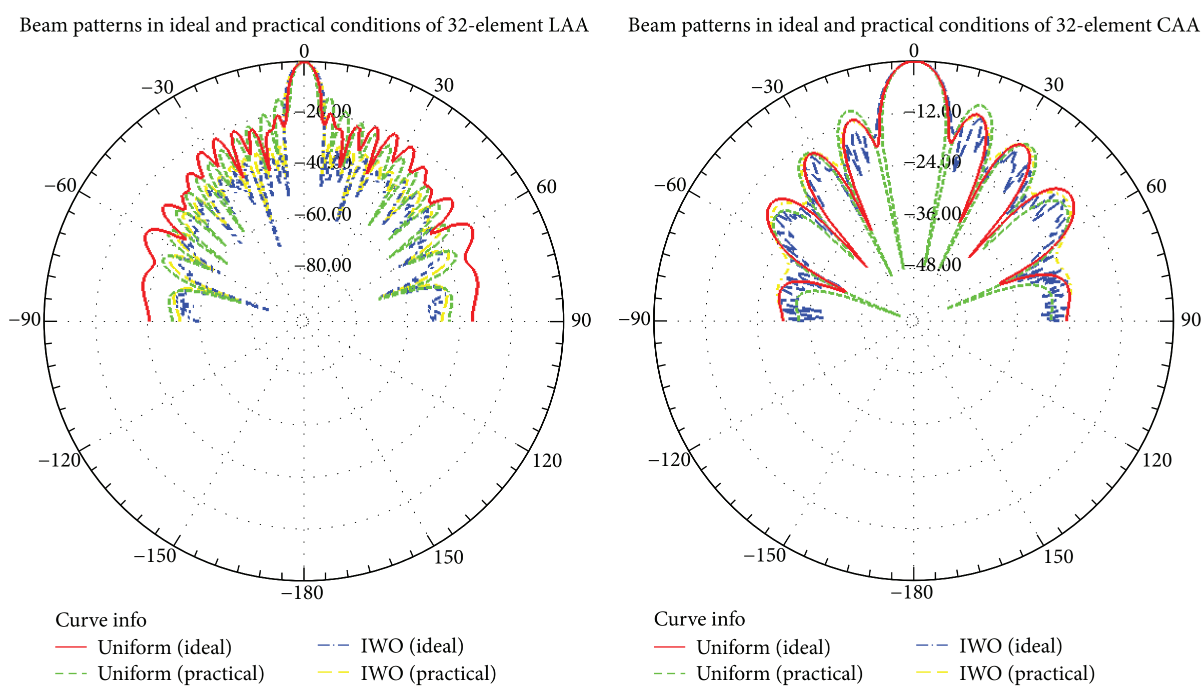

(a) (b)

Figure 19: Beam patterns obtained by uniform excitation currents and IWO in ideal and practical conditions with EM simulations. (a) 32-element LAA. (b) 32-element CAA.

stability performance of IWO is the best compared with other benchmark algorithms for the sidelobe reductions of both LAA and CAA.

5.5. EM Simulations. To verify the beam pattern performances of the antenna arrays obtained by IWO as well as other algorithms in practical conditions, we design the LAAs

(8-element, 16-element, and 32-element) and the CAAs (8-element, 16-element, and 32-element) for EM simulations based on ANSYS Electromagnetics 2016 (HFSS 15.0). First, a physical structure of the array element is designed and we use the element to construct the LAAs and the CAAs. Then, we use the excitation currents obtained by uniform excitations, IWO, CS, FA, BBO, and PSO from Tables 3 to 8 for the LAAs and the CAAs, respectively, to conduct the EM simulations. Figures 16(a) and 16(b) show the beam patterns of the 8-element LAA and CAA with different excitation currents obtained by uniform excitations, IWO, CS, FA, BBO, and PSO, respectively. It can be seen from the figures that all of the optimization algorithms can reduce the maximum SLL compared with the uniform excitation method. However, IWO achieves the lowest maximum SLL among other methods. Figures 17(a) and 17(b) show the beam patterns of the 16-element LAA and CAA obtained by different algorithms. Figures 18(a) and 18(b) show the optimization results of EM simulation for the 32-element LAA and CAA, respectively. As can be seen, similar with cases of the 8-element LAA and CAA, the beam patterns obtained by IWO also have the lowest maximum SLL with a high number of antenna elements. Therefore, IWO has a better performance for reducing the maximum SLLs of the LAAs and the CAAs in practical conditions.

Moreover, to verify the differences of the beam patterns caused by the mutual coupling, we compare the results obtained by the model used for optimization and the EM model. Figures 19(a) and 19(b) show the beam patterns obtained by the uniform excitation currents and by IWO in ideal (the array model used for optimization and simulation) and practical (the array model used for EM simulation) conditions with EM simulations. As can be seen, the beam patterns of the practical condition are distorted compared to the ideal beam patterns. Moreover, the maximum SLLs of practical condition in EM simulation are higher than that in ideal condition obtained by Matlab. Thus, the mutual coupling affects the beam pattern performance. However, the IWO algorithm is still able to provide improvement for reducing the maximum SLL in practical conditions with mutual coupling.

6. Conclusion

In this paper, the IWO algorithm is used to solve the beam pattern synthesis problem of the LAA and the CAA. We formulate an optimization problem for this goal and use IWO as the optimizer to determine a set of optimal excitation currents to achieve the desired beam patterns. Six samples including 8-element, 16-element, and 32-element LAAs and CAAs are conducted to verify the optimization performances of the SLL reductions. Simulation results show that the SLLs can be effectively reduced by IWO. Moreover, compared with other benchmark algorithms, IWO has a better performance in terms of the accuracy, the convergence rate, and the stability. In addition, EM simulation results demonstrate that the optimization results obtained by IWO are also effective for the antenna arrays in practical conditions.

Conflicts of Interest

The authors declare that they have no conflicts of interest.

Acknowledgments

This work was supported by the National Natural Science Foundation of China (Grant no. 61373123), the Chinese Scholarship Council (no. [2016] 3100), and the Graduate Innovation Fund of Jilin University (2017016).

References

[1] S. Liang, T. Feng, and G. Sun, "Sidelobe-level suppression for linear and circular antenna arrays via the cuckoo search–chicken swarm optimisation algorithm," *IET Microwaves, Antennas & Propagation*, vol. 11, no. 2, pp. 209–218, 2016.

[2] I. F. Akyildiz, S. Nie, S. C. Lin, and M. Chandrasekaran, "5G roadmap: 10 key enabling technologies," *Computer Networks*, vol. 106, pp. 17–48, 2016.

[3] D. Z. Zhu, P. L. Werner, and D. H. Werner, "Design and optimization of 3-D frequency-selective surfaces based on a multiobjective lazy ant colony optimization algorithm," *IEEE Transactions on Antennas & Propagation*, vol. 65, no. 12, pp. 7137–7149, 2017.

[4] G. Sun, Y. Liu, S. Liang, A. Wang, and Y. Zhang, "Beam pattern design of circular antenna array via efficient biogeography-based optimization," *AEU-International Journal of Electronics and Communications*, vol. 79, pp. 275–285, 2017.

[5] G. Sun, Y. H. Liu, J. Zhang, A. M. Wang, and X. Zhou, "Node selection optimization for collaborative beamforming in wireless sensor networks," *Ad Hoc Networks*, vol. 37, pp. 389–403, 2016.

[6] G. Sun, Y. H. Liu, A. M. Wang, J. Zhang, X. Zhou, and Z. Liu, "Sidelobe control by node selection algorithm based on virtual linear array for collaborative beamforming in WSNs," *Wireless Personal Communications*, vol. 90, no. 3, pp. 1443–1462, 2016.

[7] H. Li, Y. Liu, G. Sun, A. Wang, and S. Liang, "Beam pattern synthesis based on improved biogeography-based optimization for reducing sidelobe level," *Computers & Electrical Engineering*, vol. 60, pp. 161–174, 2017.

[8] S. Jayaprakasam, S. K. A. Rahim, C. Y. Leow, T. O. Ting, and A. Eteng, "Multiobjective beampattern optimization in collaborative beamforming via NSGA-II with selective distance," *IEEE Transactions on Antennas and Propagation*, vol. 65, no. 5, pp. 2348–2357, 2017.

[9] M. Fakharzadeh, S. H. Jamali, S. Safavi-Naeini, and P. Mousavi, "A fast calibration algorithm for phased array antennas based on a modified perturbation method," in *2006 IEEE Antennas and Propagation Society International Symposium*, pp. 3343–3346, Albuquerque, NM, USA, July 2006.

[10] B. K. Lau and Y. H. Leung, "A Dolph-Chebyshev approach to the synthesis of array patterns for uniform circular arrays," in *2000 IEEE International Symposium on Circuits and Systems. Emerging Technologies for the 21st Century. Proceedings (IEEE Cat No.00CH36353)*, vol. 1, pp. 124–127, Geneva, Switzerland, Switzerland, May 2000.

[11] M. A. Sarker, M. S. Hossain, and M. S. Masud, "Robust beamforming synthesis technique for low side lobe level using taylor excited antenna array," in *2016 2nd International Conference*

on Electrical, Computer & Telecommunication Engineering (ICECTE), pp. 1–4, Rajshahi, Bangladesh, December 2016.

[12] S. Todnatee and C. Phongcharoenpanich, "Iterative GA optimization scheme for synthesis of radiation pattern of linear array antenna," *International Journal of Antennas and Propagation*, vol. 2016, Article ID 7087298, 8 pages, 2016.

[13] V. Chakravarthy and P. M. Rao, "Circular array antenna optimization with scanned and unscanned beams using novel particle swarm optimization," *Indian Journal of Applied Research*, vol. 5, no. 4, 2015.

[14] G. Ram, D. Mandal, R. Kar, and S. P. Ghoshal, "Pencil beam pattern synthesis of time-modulated concentric circular antenna array using PSO with aging leader and challenger," *Journal of Electromagnetic Waves and Applications*, vol. 29, no. 12, pp. 1610–1629, 2015.

[15] A. Sharaqa and N. Dib, "Circular antenna array synthesis using firefly algorithm," *International Journal of RF and Microwave Computer-Aided Engineering*, vol. 24, no. 2, pp. 139–146, 2014.

[16] U. Singh and R. Salgotra, "Synthesis of linear antenna array using flower pollination algorithm," *Neural Computing and Applications*, vol. 29, no. 2, pp. 435–445, 2018.

[17] P. Saxena and A. Kothari, "Optimal pattern synthesis of linear antenna array using grey wolf optimization algorithm," *International Journal of Antennas and Propagation*, vol. 2016, Article ID 1205970, 11 pages, 2016.

[18] G. Sun, Y. Liu, Z. Chen, Y. Zhang, A. Wang, and S. Liang, "Thinning of concentric circular antenna arrays using improved discrete cuckoo search algorithm," in *2017 IEEE Wireless Communications and Networking Conference (WCNC)*, pp. 1–6, San Francisco, CA, USA, March 2017.

[19] G. Sun, Y. Liu, J. Li, Y. Zhang, and A. Wang, "Sidelobe reduction of large-scale antenna array for 5G beamforming via hierarchical cuckoo search," *Electronics Letters*, vol. 53, no. 16, pp. 1158–1160, 2017.

[20] A. Boldini, C. A. Gonano, F. Grimaccia et al., "Planar array optimization by means of SNO and StudGA," in *IEEE Antennas and Propagation Society International Symposium (APSURSI)*, pp. 1950-1951, Memphis, TN, USA, July 2014.

[21] P. Saxena and A. Kothari, "Ant lion optimization algorithm to control side lobe level and null depths in linear antenna arrays," *Aeu-International Journal of Electronics and Communications*, vol. 70, no. 9, pp. 1339–1349, 2016.

[22] S. Jayaprakasam, S. Rahim, and C. Y. Leow, "PSOGSA-explore: a new hybrid metaheuristic approach for beampattern optimization in collaborative beamforming," *Applied Soft Computing*, vol. 30, pp. 229–237, 2015.

[23] U. Singh, R. Salgotra, and M. Rattan, "A novel binary spider monkey optimization algorithm for thinning of concentric circular antenna arrays," *Iete Journal of Research*, vol. 62, no. 6, pp. 736–744, 2016.

[24] A. R. Mehrabian and C. Lucas, "A novel numerical optimization algorithm inspired from weed colonization," *Ecological Informatics*, vol. 1, no. 4, pp. 355–366, 2006.

[25] A. Sharaqa and N. Dib, "Design of linear and elliptical antenna arrays using biogeography based optimization," *Arabian Journal for Science and Engineering*, vol. 39, no. 4, pp. 2929–2939, 2014.

[26] D. Simon, "Biogeography-based optimization," *IEEE Transactions on Evolutionary Computation*, vol. 12, no. 6, pp. 702–713, 2008.

[27] X.-S. Yang and S. Deb, "Cuckoo search via Lévy flights," in *2009 World Congress on Nature & Biologically Inspired Computing (NaBIC)*, pp. 210–214, Coimbatore, India, December 2009.

[28] X.-S. Yang, "Firefly algorithms for multimodal optimization," in *International Symposium on Stochastic Algorithms*, pp. 169–178, Springer, 2009.

[29] J. Kennedy, "Particle swarm optimization," in *Encyclopedia of Machine Learning*, Springer, 2011.